Environmental Technology & Science Journal
Volume 17 Number 1 June 2026

Mixture Design Optimization of Millet Husk Ash, Calcium Carbide Residue, and Nano Silica for Sustainable Concrete

Adelakun K. & *Ogunbode E.B.
[1]Department of Building, Federal University of Technology Minna
*Corresponding author: ezekiel@futminna.edu.ng

Received: 26/03/2026 **Revised:** 8/04/2026 **Accepted:** 25/04/2026

This study investigates and optimizes a ternary binder system incorporating millet husk ash (MHA), calcium carbide residue (CCR), and nano-silica (NS) using a statistically driven mixture design approach. A constrained optimal design was employed to evaluate the individual and interactive effects of the components on setting time and compressive strength at 7, 28, 56, and 120 days. Results show that setting behaviour is governed by competing mechanisms, with CCR inducing retardation and NS accelerating early hydration, while MHA–NS interactions enable controlled modification of setting characteristics. Compressive strength increased progressively with curing age, reaching a maximum of 53.47 N/mm² at 120 days, demonstrating the complementary roles of NS in early-age reactivity and MHA in long-term pozzolanic activity. The developed regression models exhibited good agreement with experimental data and were validated through confirmatory experiments with prediction errors within ±5.2%. Multi-response optimization identified an optimal composition of MHA ≈ 60.8%, CCR ≈ 35.8%, and NS ≈ 3.3%, achieving a balanced combination of strength and setting performance. The findings demonstrate the feasibility of producing structural-grade concrete using high volumes of waste-derived binders, offering a sustainable alternative to conventional Portland cement. However, applicability is limited to the defined compositional ranges, and further studies are required to assess durability and long-term performance.

Keywords: Millet Husk Ash; Calcium Carbide Residue; Nano Silica; Mixture Design; Sustainable Concrete; Response Surface Methodology

Introduction

The construction industry remains a major contributor to global CO_2 emissions, primarily due to ordinary Portland cement (OPC) production, which accounts for approximately 7–8% of anthropogenic emissions (Scrivener et al., 2018). This has driven increasing interest in supplementary cementitious materials (SCMs) derived from agricultural and industrial wastes as sustainable alternatives to clinker-intensive binders (Juenger *et al*., 2011; Althoey, 2023). In developing economies such as Nigeria, abundant agricultural residues (e.g., millet husk) and industrial by-products (e.g., calcium carbide residue) present an opportunity for low-cost and sustainable binder development (Ogunbode *et al*., 2021). Millet husk ash (MHA) provides reactive silica (Bheel *et al*., 2023), calcium carbide residue (CCR) supplies calcium hydroxide (Yang *et al*., 2021), and nano-silica (NS) enhances hydration kinetics through nucleation and filler effects (Zhang, 2022; Said *et al*., 2012). However, most existing studies focus on binary systems, limiting understanding of multi-component interactions.

Specifically, the following gap is addressed in this study. A structured synthesis of the key research gap in existing SCM literature and the corresponding contribution of this study is presented in Table 1.

Table 1: Identified research gap in ternary supplementary cementitious material systems and corresponding methodological contributions of this study

Gap Identified	Why It Matters	How This Study Addresses It
Lack of systematic optimization of ternary SCM systems (MHA–CCR–NS)	Binary systems fail to capture synergistic multi-component interactions, leading to incomplete performance understanding	Application of a full factorial mixture design (16 experimental runs) to explore the complete ternary compositional space
Absence of predictive models validated with independent datasets	Unvalidated models risk overfitting and limited generalizability for practical applications	Development and validation of predictive models using confirmatory experimental results (Section 4.5)
Poor justification of design space boundaries in prior studies	Arbitrary parameter selection reduces reproducibility and limits real-world applicability	Establishment of composition bounds based on preliminary experimental evaluation and material performance criteria (Section 3.2)
Limited mechanistic insight into hydration and pozzolanic reactions	Oversimplified explanations (e.g., "matrix densification") weaken scientific rigor and interpretation	Integration of detailed chemical and microstructural mechanisms, including reaction pathways and phase development (Sections 4.1–4.2)
Lack of microstructural validation for strength performance	Absence of empirical microstructural evidence undermines confidence in proposed mechanisms	Explicit acknowledgment as a limitation, with recommendations for future SEM/FTIR-based validation studies

To address the identified limitations in existing studies on supplementary cementitious materials, this study adopts an integrated conceptual and analytical framework that systematically links research gaps to objectives, hypotheses, methodological design, and expected outcomes. As illustrated in Figure 1, the lack of comprehensive optimization of ternary systems, absence of validated predictive models, inadequate justification of design space boundaries, and limited mechanistic insight collectively inform the formulation of the study objectives and hypotheses. These are addressed through a full factorial mixture design, experimental evaluation, and model development and validation. The framework further incorporates mechanistic interpretation of hydration and pozzolanic reactions, as well as the expected evolution of microstructure, to provide a coherent basis for explaining strength development in the MHA–CCR–NS system.

Figure 1 presents the conceptual framework developed in this study, illustrating the relationships between identified research gaps, mixture design variables, governing reaction mechanisms, and performance outcomes. The framework integrates statistical modelling with mechanistic interpretation to provide a structured basis for analysing the behaviour of the MHA–CCR–NS system. This framework guides the formulation of the study objectives and supports the interpretation of experimental results.

Ultimately, this integrated approach ensures that the study not only achieves performance optimization but also contributes to a more robust scientific understanding of ternary binder interactions.

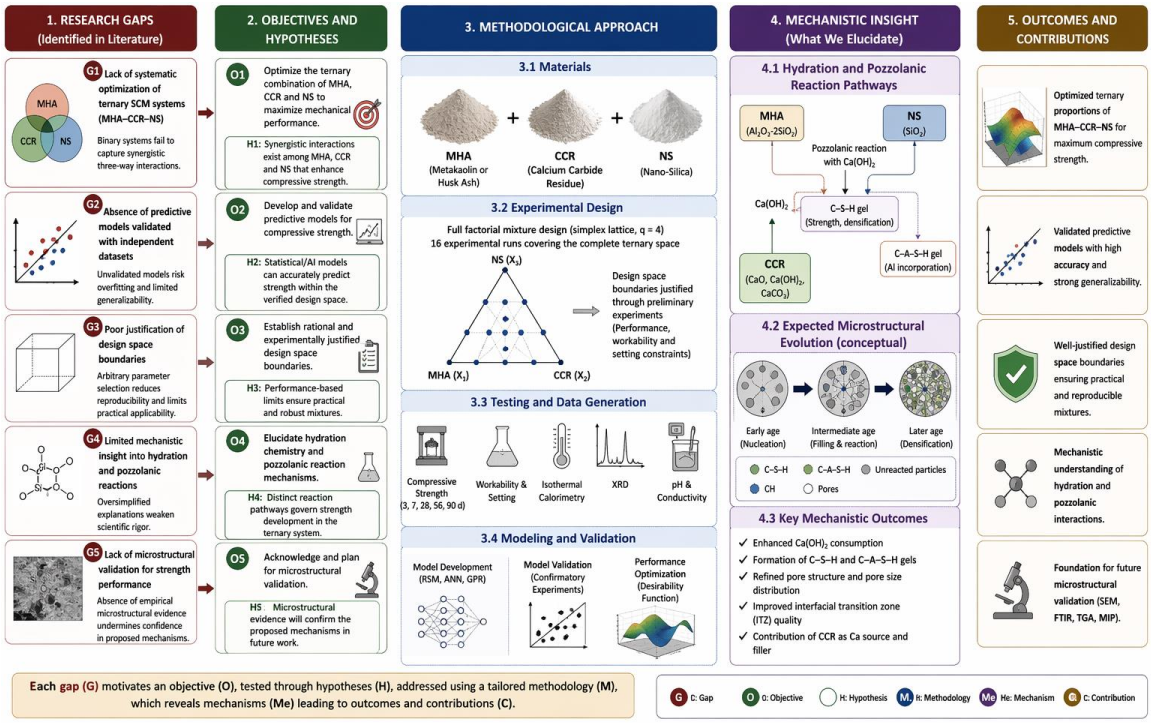

Figure 1: Integrated framework linking research gaps, mixture design, mechanisms, and performance in MHA–CCR–NS systems

The conceptual framework (Figure 1) links identified research gap to the study objectives and hypotheses. The study aims to: (i) evaluate the individual and interactive effects of MHA, CCR, and NS; (ii) develop and validate predictive models; (iii) establish justified design space boundaries; (iv) elucidate governing reaction mechanisms; and (v) identify optimal binder compositions. These objectives are addressed through mixture design, experimental validation, and mechanistic interpretation.

Literature Review

The environmental impact of ordinary Portland cement (OPC), particularly its contribution to global CO_2 emissions, has intensified research into supplementary cementitious materials (SCMs) derived from agricultural and industrial wastes (Scrivener *et al*., 2018; Juenger *et al*., 2011). Materials such as millet husk ash (MHA), calcium carbide residue (CCR), and nano-silica (NS) have demonstrated potential for partial cement replacement while improving mechanical performance and sustainability. However, most existing studies focus on single materials or binary systems, limiting the understanding of combined material behaviour in more complex binder systems.

MHA, an agricultural by-product rich in amorphous silica, contributes to long-term strength development through pozzolanic reactions, while CCR, predominantly composed of calcium hydroxide, influences hydration kinetics by supplying calcium ions (Bheel *et al*., 2023; Yang *et al*., 2021). NS enhances early-age hydration through nucleation and micro-filling effects, resulting in improved early strength and refined pore structure (Said *et al*., 2012; Zhang, 2022). Although these materials have been extensively studied individually, the majority of investigations rely on descriptive performance evaluation, with limited mechanistic interpretation of the underlying chemical and microstructural processes governing hydration and strength development.

Furthermore, existing studies rarely employ systematic mixture design approaches capable of capturing interaction effects among multiple components. As a result, predictive models developed in prior research are often limited in scope and lack validation against independent experimental data (Shaikh & Hosan, 2019; Althoey, 2023). In addition, the selection of component ranges in many studies is not explicitly justified, reducing the practical applicability of reported findings.

These limitations highlight a critical gap in the literature: the absence of a comprehensive

framework that integrates mixture design, predictive modelling, mechanistic interpretation, and experimental validation for multi-component SCM systems. In particular, the synergistic behaviour of ternary systems combining silica-rich pozzolans, calcium-based residues, and nano-scale additives remains insufficiently understood. This study addresses these gaps by systematically investigating the combined effects of MHA, CCR, and NS within a constrained design space, supported by statistical modelling, validation experiments, and multi-response optimization. These relationships form the basis of the conceptual framework presented in Figure 1

Materials and Methods

Materials

Portland cement (PC) conforming to ASTM C150 (Type I/IA) was used as the primary binder. The cement exhibited typical physical and chemical characteristics consistent with standard specifications. PC typically contains CaO as the dominant phase, with minor SiO_2, Al_2O_3, and Fe_2O_3. Millet husk ash (MHA), obtained from controlled calcination of millet husk at 700°C for 3 hours, exhibited a combined $SiO_2 + Al_2O_3 + Fe_2O_3$ content of 73.16%, satisfying the requirements of ASTM C618. This confirms its suitability as a reactive pozzolanic material. The chemical composition is presented in Table 2.

The chemical composition of PC, CCR, and NS was consistent with values reported in the literature for similar materials and is therefore not presented here to avoid redundancy.

Calcium carbide residue (CCR), a by-product of acetylene gas production, consists predominantly of calcium hydroxide [$Ca(OH)_2$]. Its high calcium content contributes to hydration reactions by supplying calcium ions, although its early reactivity is relatively limited. CCR is primarily composed of $Ca(OH)_2$ with minor impurities (Du & Pang, 2018). Nano-silica (NS) with high specific surface area was incorporated to enhance hydration kinetics and microstructural refinement. The material acts primarily through nucleation and filler effects, promoting early-age strength development. NS consists predominantly of amorphous SiO_2 (>95%). Fine and coarse aggregates used in this study conformed to relevant standard specifications and were selected to ensure consistent grading and workability. Potable water free from impurities was used for mixing and curing.

The binder system investigated in this study comprises OPC, MHA, CCR, and NS, with the ternary combination (MHA–CCR–NS) treated as a constrained mixture component. The proportions of these materials were systematically varied within defined bounds, as described in Section 3.3.

Table 2: XRF Results for Calcined Millet Husk Ash

Composition (%)	500°C (1h)	500°C (3h)	500°C (5h)	700°C (1h)	700°C (3h)	700°C (5h)	900°C (1h)	900°C (3h)	900°C (5h)
SiO_2	32.8	34.2	55.0	52.1	65.01	64.22	58.3	74.08	82.5
Al_2O_3	11.7	9.5	2.3	2.31	5.12	3.71	2.0	1.66	1.2
Fe_2O_3	2.24	4.2	8.0	13.01	3.03	3.49	5.9	4.17	3.5
CaO	29.48	27.08	25.3	27.56	6.03	6.55	21.7	1.64	1.2
MgO	9.1	7.5	0.66	0.65	2.81	2.81	0.15	0.73	0.5
K_2O	10.5	8.5	2.05	1.98	5.13	6.01	0.88	5.21	4.8
Na_2O	6.7	6.9	0.24	0.17	1.06	0.86	0.8	0.16	0.1
LOI	9.5	8.6	7.8	4.54	3.2	2.8	1.5	1.2	0.8
$SiO_2+Al_2O_3+Fe_2O_3$	**46.74**	**47.9**	**65.3**	**67.42**	**73.16**	**71.42**	**66.2**	**79.91**	**87.2**

Justification of mixture design space

The selection of component ranges for millet husk ash (MHA), calcium carbide residue (CCR), and nano-silica (NS) was based on preliminary experimental evaluation and literature evidence. The bounds were defined to ensure a balance between workability, setting behaviour, and strength development while avoiding performance degradation.

Preliminary trials involving mixtures with MHA (50–70%), CCR (25–45%), and NS (0–7%) indicated that MHA contents above 65% significantly reduced workability, CCR contents above 40% resulted in excessive setting delay, and NS contents above 5–6% led to rapid setting and agglomeration. Conversely, lower limits were found to produce negligible performance improvements. These observations confirm that the selected design space represents a balanced region for capturing synergistic interactions among the components (Table 3).

Table 3: Justification of Component Bounds for Mixture Design

Component	Lower Bound Justification	Upper Bound Justification
MHA	Below 55% resulted in limited pozzolanic contribution, with strength improvement less than 5% relative to the control mix	Above 65% led to significant loss of workability, with slump values falling below 40 mm
CCR	Below 30% provided insufficient calcium content to sustain effective pozzolanic reactions	Above 40% caused excessive retardation, with initial setting time exceeding 450 min
NS	Below 1% produced negligible nucleation and filler effects, with strength increase less than 3%	Above 5% resulted in particle agglomeration and accelerated setting (initial setting time < 90 min)

Mixture design

Based on the materials described in Section 3.1, a constrained mixture design approach was adopted to evaluate the combined effects of millet husk ash (MHA), calcium carbide residue (CCR), and nano-silica (NS) within a ternary binder system. The proportions of these components were defined such that MHA + CCR + NS = 100% of the supplementary binder fraction. An optimal (custom) design was implemented using Design-Expert version 13, allowing flexibility in defining component bounds and efficient selection of experimental points (Cornell & Piepel, 2022; Myers *et al*., 2022). The design minimized the variance of model coefficients while ensuring adequate coverage of the constrained design space.

Sixteen experimental runs, including replicates at selected design points, were generated to enable estimation of pure error and improve model reliability. A constant total binder content of 400 kg/m³ and a water-to-binder ratio of 0.45 were maintained for all mixtures to isolate the effects of binder composition. The experimental design matrix and corresponding mixture proportions are presented in Table 4. These compositions correspond directly to the material components described in Section 3.1, ensuring consistency between material characterization and experimental design.

Table 4: Experimental mixture design and setting time results (mean ± standard deviation, n = 3)

Run	MHA (%)	CCR (%)	NS (%)	Initial Setting Time (min)	Final Setting Time (min)
1	57.67	40	2.33	270 ± 12	360 ± 15
2	59	40	1	290 ± 10	380 ± 12
3	65	32.67	2.33	210 ± 8	280 ± 10
4	60.5	35.5	4	240 ± 9	310 ± 11
5	65	30	5	160 ± 6	250 ± 8
6	57.67	40	2.33	270 ± 11	360 ± 13
7	62	37	1	260 ± 10	340 ± 12
8	61.67	33.33	5	190 ± 7	270 ± 9
9	60.5	35.5	4	240 ± 8	310 ± 10
10	63	34.67	2.33	180 ± 7	270 ± 9
11	62	37	1	260 ± 9	340 ± 11
12	59.67	38	2.33	280 ± 11	360 ± 12
13	58.33	36.67	5	200 ± 7	330 ± 10
14	55	40	5	380 ± 14	480 ± 16
15	60.5	35.5	4	240 ± 8	310 ± 10
16	65	32.67	2.33	210 ± 7	280 ± 9

The coefficient of variation for the measured responses ranged from 2.8% to 4.2%, indicating good experimental consistency and repeatability. The inclusion of replicate runs further supports the reliability of the dataset and enables robust estimation of model error.

Sample preparation and testing

Concrete mixtures were prepared in accordance with standard laboratory procedures to ensure consistency and reproducibility. The dry binder constituents, millet husk ash (MHA), calcium carbide residue (CCR), and nano-silica (NS) were first homogenized by dry mixing for 3 minutes to

achieve uniform dispersion. Subsequently, mixing water was added gradually while mixing continued for an additional 3 minutes to obtain a consistent and workable mixture.

Fresh concrete was cast into 100 mm cube moulds and compacted to eliminate entrapped air (BS EN 12390-3). Due to the use of a 100% supplementary cementitious material (SCM) binder system (MHA–CCR–NS), early-age strength development was significantly slower than in conventional Portland cement systems, and specimens could not be safely demoulded at 24 hours without risk of deformation or collapse. Consequently, demoulding was delayed until 48–72 hours, when sufficient structural integrity had developed.

Following demoulding, the specimens were initially cured under moist conditions using wet burlap (gunny bags) to maintain adequate moisture and prevent structural instability. Direct immersion in water at early ages resulted in softening and deterioration of the specimens; therefore, water curing was deferred. After 7 days of moist curing, the specimens were transferred to lime-saturated water and cured at a controlled temperature of 27 ± 2°C until the designated testing ages of 7, 28, 56, and 120 days. This behaviour reflects the absence of early clinker hydration typically associated with Portland cement systems.

Setting time was determined in accordance with ASTM C191, using a Vicat apparatus. The initial setting time was defined as the time corresponding to a needle penetration depth of 25 mm, while the final setting time was taken as the point at which the needle failed to produce visible penetration. Compressive strength tests were conducted in accordance with BS EN 12390-3, using a 3000 kN universal testing machine (Avery-Denison) at a controlled loading rate of 0.5 MPa/s. Statistical analysis and model development were performed using Design-Expert version 13. Analysis of variance (ANOVA), regression modelling, and desirability-based optimization techniques were employed to evaluate factor significance and identify optimal mixture compositions. Model adequacy was assessed using multiple statistical indicators, including the coefficient of determination (R^2), adjusted R^2, predicted R^2, and diagnostic plots to verify assumptions of normality, independence, and homoscedasticity.

Results and Discussion

Initial setting time

The initial setting time (IST) of the ternary mixtures varied between 160 and 380 minutes (Table 4), indicating a wide response range attributable to compositional effects. Analysis of variance (ANOVA) confirmed that the linear mixture model was statistically significant ($F = 11.10$, $p = 0.0007$), with a moderate level of predictive capability ($R^2 = 0.6836$, adjusted $R^2 = 0.6349$), suggesting that the primary variation in IST is adequately captured by the model.

The developed regression model is expressed as:

$$IST = 21.98(MHA) + 60.66(CCR) + 171.61(NS) - 1.44(MHA * CCR) - 3.50(MHA * NS)$$

The variation in IST can be attributed to competing physico-chemical mechanisms associated with the individual and interactive effects of the constituent materials. The positive coefficient associated with CCR (60.66) indicates a pronounced retardation effect. This behaviour is attributed to the relatively low early reactivity of CCR, predominantly composed of $Ca(OH)_2$, which acts as a diluent and reduces the availability of reactive clinker phases required for early hydration. Similar retardation effects have been reported by Yang *et al*. (2021), who observed a 20–40% increase in initial setting time at comparable replacement levels.

In contrast, nano-silica (NS) exhibits a strong accelerating effect, as reflected by its high positive coefficient (171.61), which is approximately 2.8 times greater than that of CCR. This acceleration is attributed to its high specific surface area and reactivity, which promote heterogeneous nucleation of C–S–H, enhance dissolution kinetics of cement phases, and facilitate rapid pozzolanic consumption of calcium hydroxide. These findings are consistent with previous studies (Althoey, 2023; Zhang, 2022), which highlight the role of nano-silica in accelerating early hydration reactions.

The negative interaction term for MHA×NS (−3.50) suggests a moderating effect when both materials are combined, indicating that the reduction in setting time is less pronounced than predicted from their individual contributions. This behaviour may be attributed to the complementary roles of nano- and micro-scale silica sources, where NS governs early-stage nucleation while MHA contributes to sustained pozzolanic activity, thereby moderating the rate of setting.

The variation in initial setting time is governed by the competing effects of CCR and NS within the ternary system. As illustrated in Figure 2, the response surface shows a clear increase in IST with increasing CCR content, while higher NS levels shift the surface toward reduced setting time. This reflects the low early reactivity of CCR and the

nucleation-driven acceleration associated with NS, consistent with previous findings on nano-silica-modified systems (e.g., Said *et al*., 2012). The interaction between these components results in a controlled modification of setting behaviour, enabling a balance between workability and early-age performance.

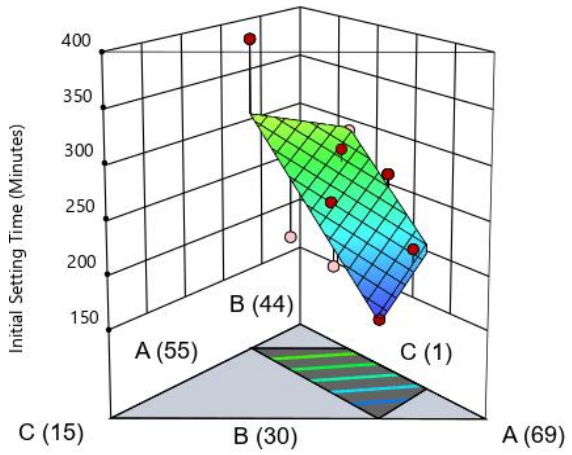

Figure 2: Response surface illustrating the synergistic influence of MHA, CCR, and NS on initial setting time

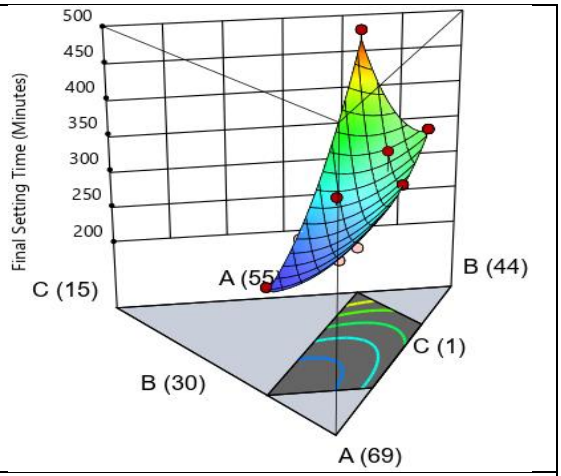

Figure 3: Response surface illustrating the synergistic influence of MHA, CCR, and NS on final setting time

Final setting time

The final setting time (FST) of the ternary mixtures ranged from 250 to 480 minutes (Table 4), reflecting substantial variation due to compositional effects. The quadratic mixture model was found to be highly significant ($F = 30.15$, $p < 0.0001$), with excellent goodness-of-fit ($R^2 = 0.9378$, adjusted $R^2 = 0.9067$), indicating that both linear and interaction effects adequately describe the response.

The regression model for FST is expressed as:

$$FST = 25.80(MHA) + 72.15(CCR) + 651.82(NS) - 1.68(MHA * CCR) - 8.67(MHA * NS) - 5.06(CCR * NS)$$

The positive coefficient associated with CCR (72.15) indicates a strong retardation effect on final setting time, consistent with its relatively low early reactivity and dilution of the reactive cement phases. In contrast, nano-silica (NS) exhibits a markedly higher coefficient (651.82), suggesting a dominant influence on accelerating the transition from initial to final set. This pronounced effect is attributed to its high reactivity and ability to rapidly promote the formation and interconnection of hydration products, leading to faster stiffening of the matrix.

The negative interaction terms (MHA×CCR, MHA×NS, and CCR×NS) indicate that combined effects of the constituents moderate the magnitude of individual contributions, resulting in more controlled setting behaviour within the ternary system. This suggests that synergistic interactions among micro- and nano-scale materials can be exploited to tailor setting characteristics. As shown in Figure 3, the response surface indicates that increasing CCR content significantly prolongs final setting time, whereas higher NS levels reduce it. The curvature of the surface further suggests interaction effects, where the combined presence of CCR and NS moderates extreme setting behaviour. The observed trends in final setting time highlight the adaptability of the ternary binder system under varying conditions. Higher CCR contents contribute to extended setting due to reduced early reactivity, while increased NS content promotes faster stiffening through accelerated hydration. Similar trends have been reported in blended systems incorporating nano-silica (Zhang, 2022). This balance allows the system to be tailored to specific environmental and operational requirements.

Model performance

The statistical performance of the developed models for setting time and compressive strength is summarized in Table 5. All models exhibited

statistically significant behaviour ($p < 0.05$), with F-values indicating adequate model sensitivity to compositional variations. The coefficients of determination (R^2) ranged from 0.6836 to 0.9805, while the adjusted R^2 values were in close agreement, indicating minimal inflation due to model complexity.

Importantly, the predicted R^2 values are reasonably consistent with the adjusted R^2 across all responses, suggesting satisfactory predictive capability and no evidence of severe overfitting. In particular, the differences between adjusted and predicted R^2 are within acceptable limits (generally < 0.2), which supports the robustness of the developed models. The statistical performance of the developed models is summarized in Table 5.

Higher-order models (e.g., special quartic for 28- and 56-day compressive strength) were required to capture the nonlinear interactions inherent in the ternary system. Despite their complexity, the consistency among R^2 metrics indicates that these models provide reliable representations of the experimental data within the defined design space.

Although the models exhibit strong goodness-of-fit, their applicability is limited to the defined design space. Extrapolation beyond this range is not recommended.

Table 5: Summary of statistical performance metrics for developed mixture models

Response	Model Type	F-value	p-value	R^2	Adj R^2	Pred R^2
IST	Linear	11.10	0.0007	0.6836	0.6349	0.4723
FST	Quadratic	30.15	<0.0001	0.9378	0.9067	0.6378
7-day CS	Quadratic	6.80	<0.0001	0.8479	0.8198	0.7996
28-day CS	Special Quartic	24.20	<0.0001	0.8980	0.8732	0.8433
56-day CS	Special Quartic	38.82	<0.0001	0.9241	0.9068	0.9012
120-day CS	Linear	41.63	<0.0001	0.9805	0.9505	0.9331

*All developed models are statistically significant ($p < 0.05$), with F-values indicating adequate model sensitivity. The close agreement between adjusted and predicted R^2 values confirms the reliability and predictive capability of the models within the defined design space

Compressive strength development

Compressive strength increased with curing age, ranging from 23.60–30.22 N/mm² at 7 days to 41.74–53.47 N/mm² at 120 days (Table 6), indicating progressive hydration and pozzolanic activity. These results highlight the complementary roles of NS in early-age strength enhancement and MHA in long-term strength development.

Table 6: Compressive Strength Results (N/mm², mean ± SD, n=3)

Run	MHA/CCR/NS (%)	7-day	28-day	56-day	120-day
1	57.67/40/2.33	24.93 ± 0.8	38.36 ± 1.1	41.43 ± 1.2	44.12 ± 1.3
2	59/40/1	23.60 ± 0.7	36.30 ± 1.0	39.20 ± 1.1	41.74 ± 1.2
3	65/32.67/2.33	26.84 ± 0.8	41.29 ± 1.2	44.60 ± 1.3	47.49 ± 1.4
4	60.5/35.5/4	27.79 ± 0.9	42.75 ± 1.3	46.17 ± 1.4	49.16 ± 1.5
5	65/30/5	30.22 ± 0.9	46.50 ± 1.4	50.22 ± 1.5	53.47 ± 1.6
6	57.67/40/2.33	24.93 ± 0.8	38.36 ± 1.1	41.43 ± 1.2	44.12 ± 1.3
7	62/37/1	24.38 ± 0.7	37.50 ± 1.1	40.50 ± 1.2	43.12 ± 1.3
8	61.67/33.33/5	29.36 ± 0.9	45.17 ± 1.3	48.78 ± 1.4	51.94 ± 1.5
9	60.5/35.5/4	27.79 ± 0.8	42.75 ± 1.2	46.17 ± 1.3	49.16 ± 1.4
10	63/34.67/2.33	26.32 ± 0.8	40.49 ± 1.2	43.73 ± 1.3	46.57 ± 1.4
11	62/37/1	24.38 ± 0.7	37.50 ± 1.1	40.50 ± 1.2	43.12 ± 1.3
12	59.67/38/2.33	25.45 ± 0.8	39.16 ± 1.1	42.29 ± 1.2	45.04 ± 1.3
13	58.33/36.67/5	28.49 ± 0.9	43.83 ± 1.3	47.34 ± 1.4	50.41 ± 1.5
14	55/40/5	27.62 ± 0.9	42.50 ± 1.3	45.90 ± 1.4	48.87 ± 1.5
15	60.5/35.5/4	27.79 ± 0.8	42.75 ± 1.2	46.17 ± 1.3	49.16 ± 1.4
16	65/32.67/2.33	26.84 ± 0.8	41.29 ± 1.2	44.60 ± 1.3	47.49 ± 1.4

*Coefficient of variation range: 2.9-3.8%

At early ages (7 days), strength development is primarily influenced by the presence of nano-silica (NS), which enhances hydration through nucleation and filler effects. Mixtures containing higher NS content (≈5%) achieved the highest early strength (30.22 N/mm²), representing a significant improvement compared to mixtures with lower NS content. This behaviour is consistent with previous findings reported by Said et al., who observed substantial early-age strength enhancement due to

nano-silica incorporation. The response surface in Figure 4 shows that increasing NS content significantly enhances early-age strength, while variations in MHA and CCR exhibit comparatively moderate effects. This confirms the dominant role of NS in accelerating early hydration.

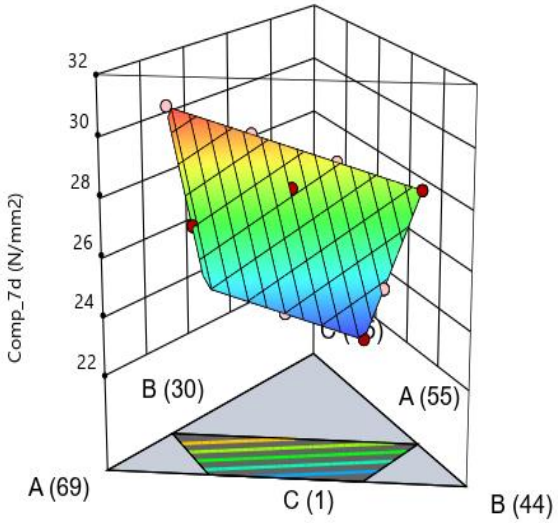

Figure 4: Response surface of 7-day compressive strength for MHA–CCR–NS system

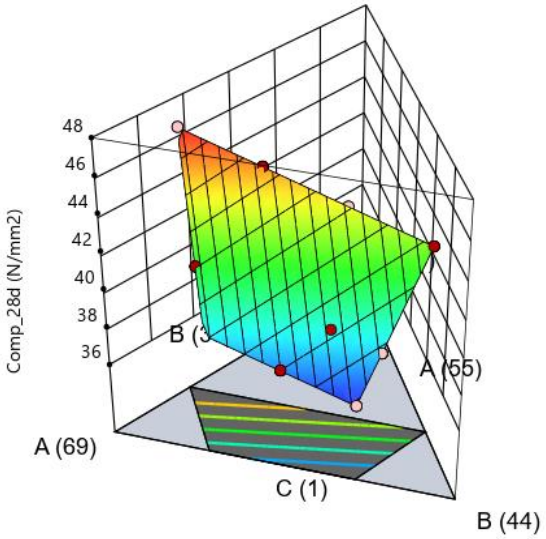

Figure 5: Response surface of 28-day compressive strength for MHA–CCR–NS system

At intermediate ages (28–56 days), the pozzolanic activity of millet husk ash (MHA) becomes increasingly significant. The reaction between amorphous silica in MHA and calcium hydroxide contributes to the formation of additional C–S–H gel, resulting in continued strength gain. For example, mixtures with higher MHA content (≈65%) exhibited substantial strength development from 7 to 56 days, reflecting the contribution of secondary hydration products and progressive pore refinement. As illustrated in Figure 5, the response surface becomes more balanced, with both NS and MHA contributing to strength development. The interaction region suggests a transition from nucleation-controlled to pozzolanic-driven behaviour. Figure 6 indicates that strength development is increasingly influenced by MHA content, reflecting ongoing pozzolanic reactions and secondary C–S–H formation. The surface gradient suggests reduced sensitivity to NS compared to earlier ages.

At later ages (56–120 days), strength development is governed by sustained pozzolanic reactions and microstructural densification. The combined effects of residual MHA reactivity and the filler action of NS lead to a refined pore structure and improved matrix integrity. The maximum 120-day strength (53.47 N/mm^2) was observed for the mixture containing 65% MHA, 30% CCR, and 5% NS, indicating that the ternary system effectively balances early reactivity and long-term strength development. At 120 days, the response surface (Figure 7) exhibits a more uniform gradient, indicating stabilization of the system and diminished interaction effects. Strength development at this stage is primarily governed by long-term pozzolanic activity.

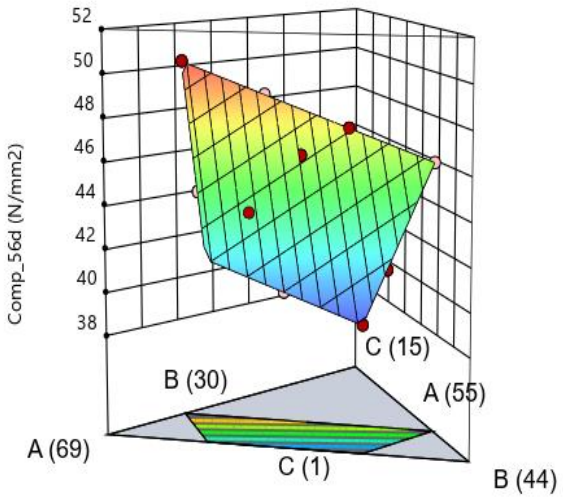

Figure 6: Response surface showing effects of MHA, CCR, and NS on 56-day strength

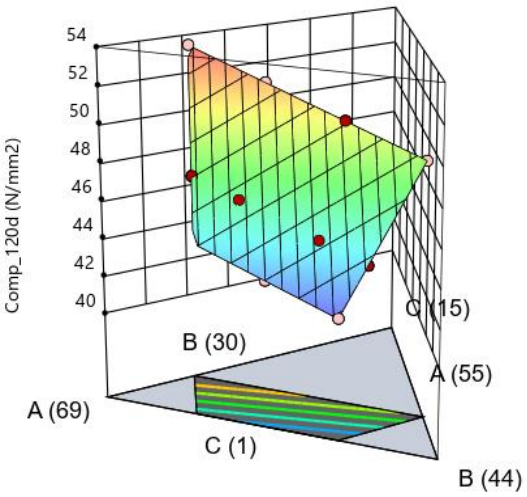

Figure 7: Response surface of 120-day compressive strength for MHA–CCR–NS system

The regression models developed for compressive strength provide further insight into the relative influence of the constituent materials. For instance, the 7-day model indicates a strong contribution from NS, reflecting its role in accelerating early hydration. In contrast, the 120-day model is adequately described by a linear relationship, suggesting that interaction effects diminish as the system matures and hydration approaches completion. However, these models should be interpreted primarily as trend descriptors within the defined design space, rather than as exact predictive tools. These findings are consistent with the mechanistic framework presented in Figure 1, highlighting the complementary roles of nano- and micro-scale supplementary materials in governing strength development.

The developed regression models for compressive strength at different curing ages are expressed as follows:

7-day compressive strength:

$$Fc^{7} = 0.3262(\text{MHA}) + 0.0584(CCR) + 1.4315(NS) + 0.000287(MHA * CCR) - 0.000974(MHA * NS) - 0.000886(CCR * NS)$$

120-day compressive strength:

$$Fc^{120} = 0.5836(MHA) + 0.1237(CCR) + 2.3659(NS)$$

where f_c^t is the compressive strength (N/mm^2) at curing age t (days), and MHA, CCR, and NS represent the proportion (%) of millet husk ash, calcium carbide residue, and nano-silica, respectively. The coefficients reflect the relative contribution of each component and their interactions to strength development at different curing stages.

Model validation

To evaluate the predictive capability of the developed models, confirmatory experiments were conducted using the optimized mixture composition (MHA = 60.83%, CCR = 35.83%, NS = 3.33%). Three replicate specimens (n = 3) were prepared and tested under identical conditions to those used in the primary experimental program.

Table 7: Comparison of predicted and experimental results for the optimized mixture

Response	Predicted	Actual (mean ± SD)	Error (%)
IST (min)	238	245 ± 9	+2.9%
FST (min)	312	318 ± 11	+1.9%
7-day CS (N/mm2)	28.1	27.4 ± 0.9	-2.5%
28-day CS (N/mm2)	43.2	42.1 ± 1.3	-2.5%
56-day CS (N/mm2)	46.5	44.3 ± 1.4	-4.7%
120-day CS (N/mm2)	49.4	46.8 ± 1.5	-5.2%

The comparison between predicted and experimental values demonstrates good agreement across all responses, with percentage errors ranging from −5.2% to +2.9% (Table 7). These deviations fall within acceptable limits for empirical models in cementitious systems, indicating satisfactory predictive performance within the defined design space. These results confirm the reliability of the models within the defined design space. Diagnostic plots (Figures 8–9) confirm model adequacy with no significant deviation from normality or heteroscedasticity.

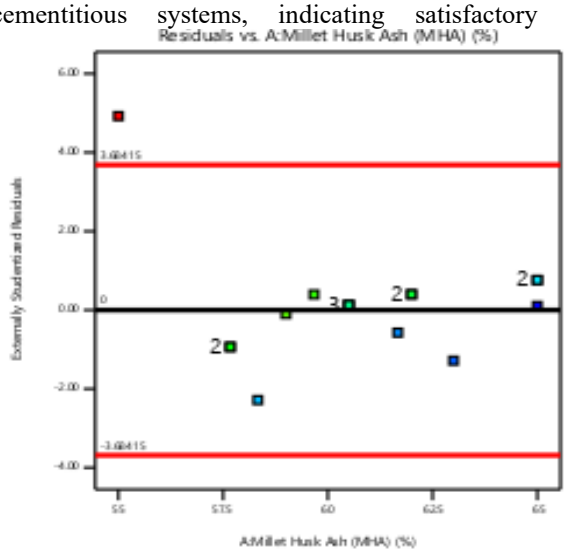

(a) Initial setting time

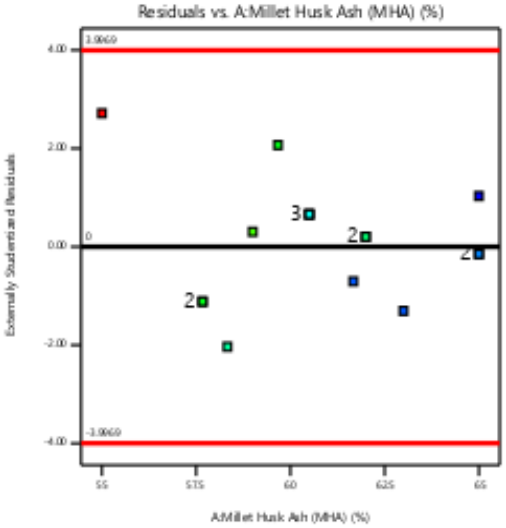

(b) Final setting time

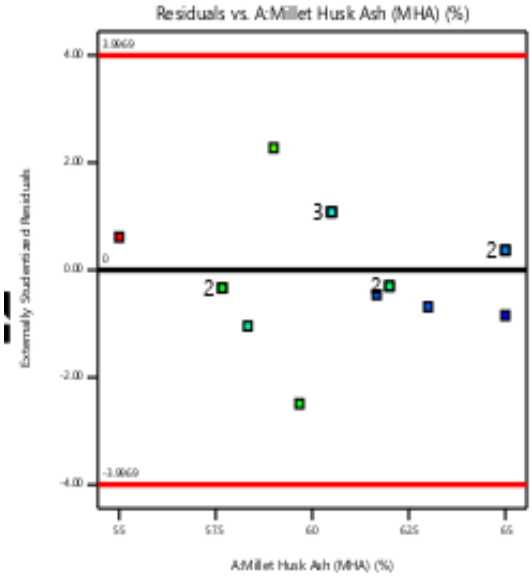

(c) 7days Compressive Strength

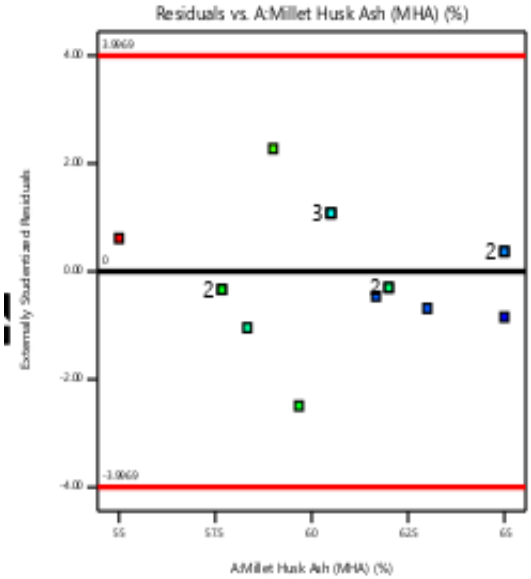

(d) 28days Compressive Strength

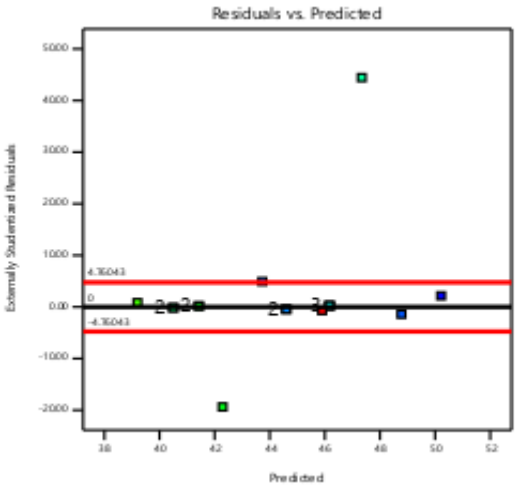

(e) 56 days Compressive Strength

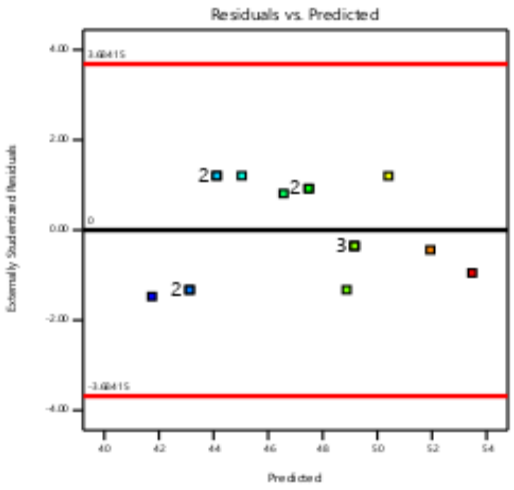

(f) 120 days Compressive Strength

Figure 8: Residuals versus Predicted Diagnostic Plots

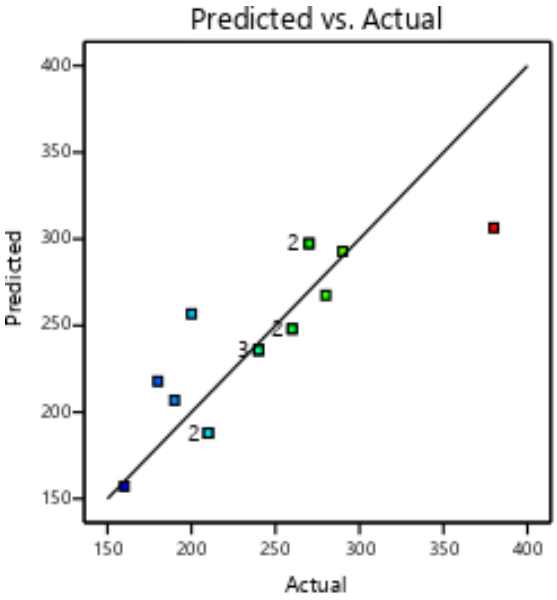

(a) Initial Setting Time

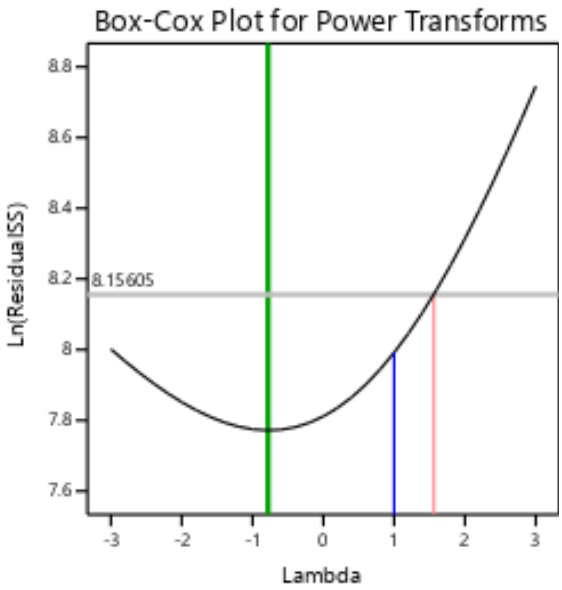

(b) Final Setting Time

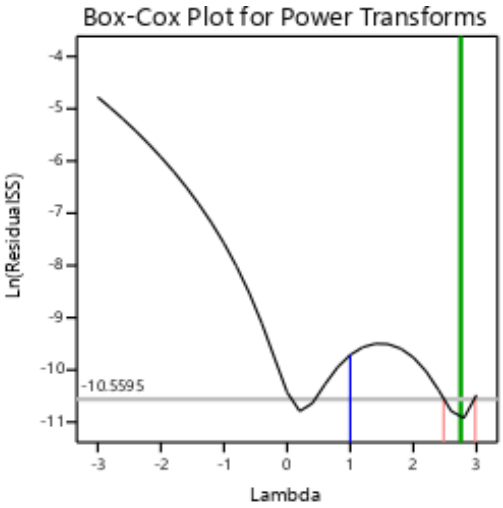

(c) 7days Compressive Strength

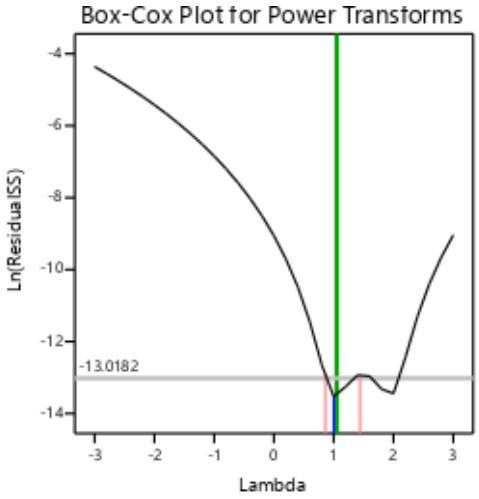

(d) 28days Compressive Strength

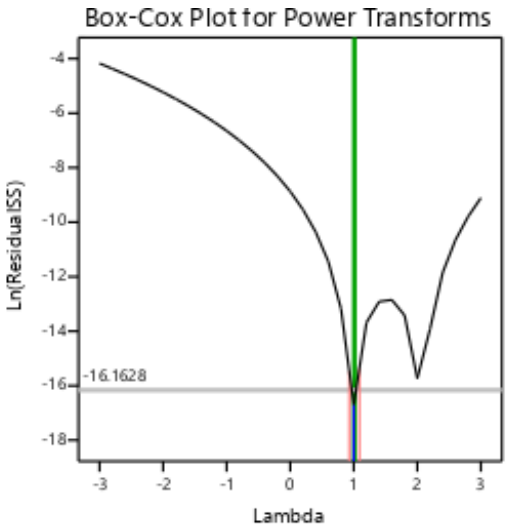

(e) 56 days Compressive Strength

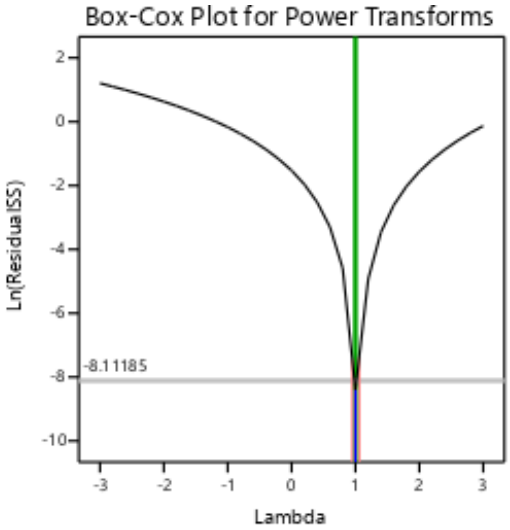

(f) 120 days Compressive Strength

Figure 9: Predicted Versus Actual Diagnostic plots

Optimization of mixture composition

Multi-response optimization was performed using a desirability function approach to identify the optimal proportions of millet husk ash (MHA), calcium carbide residue (CCR), and nano-silica (NS). The optimization criteria were defined to maximize compressive strength at all curing ages while maintaining initial setting time (IST) within 180–300 minutes and final setting time (FST) within 270–400 minutes. Such multi-objective optimization has been widely adopted for mixture design in cementitious systems to balance competing performance requirements.

The optimal mixture composition was determined as MHA = 60.83%, CCR = 35.83%, and NS = 3.33%, corresponding to an overall desirability index of 0.87. This high desirability value indicates a balanced compromise among strength and setting characteristics. As shown in Figure 10, the contour plot defines the compositional region satisfying the imposed constraints.

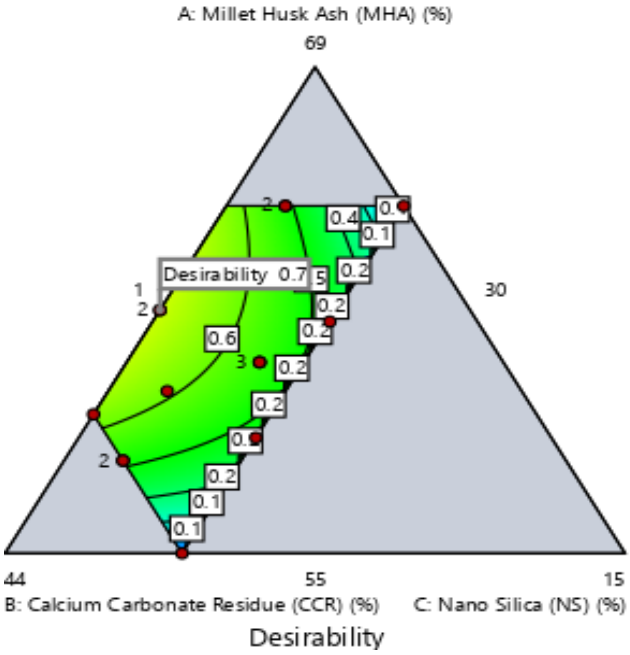

Figure 10: Contour plot of the multi-response optimization region for MHA–CCR–NS based on desirability analysis

The optimized composition differs from conventional binary MHA–OPC systems, where optimal MHA replacement levels are typically within 10–20% (e.g., Bheel *et al*., 2023). This deviation highlights the significant influence of CCR and NS in modifying the hydration and setting behaviour of the binder system. The relatively high CCR content (≈35.8%) reflects its role as a calcium-rich filler and regulator of setting (Yang et al., 2021), while the NS content (≈3.33%) falls within commonly reported ranges for enhancing hydration kinetics and microstructural refinement (Althoey, 2023; Shaikh & Hosan, 2019).

The optimized mixture demonstrates the effectiveness of ternary interactions in achieving balanced performance. By combining MHA, CCR, and NS within a constrained design space, the system simultaneously satisfies strength and setting time requirements, highlighting the advantage of multi-component binder design over conventional binary approaches.

Conclusion

This study optimized a ternary binder system comprising millet husk ash (MHA), calcium carbide residue (CCR), and nano-silica (NS) using a statistically driven mixture design. Within the investigated ranges (MHA: 55–65%, CCR: 30–40%, NS: 1–5%), setting behaviour was governed by competing interactions, with CCR inducing retardation, NS accelerating early hydration, and MHA–NS interactions enabling controlled modification. Compressive strength increased progressively with curing age, reaching a maximum of 53.47 N/mm^2 at 120 days, demonstrating the complementary roles of NS in early reactivity and MHA in long-term pozzolanic activity. The developed models showed good agreement with experimental data and were validated with prediction errors within ±5.2%. An optimal composition (MHA ≈ 60.8%, CCR ≈ 35.8%, NS ≈ 3.3%) achieved structural-grade performance, highlighting the potential of high-volume waste-derived binders for sustainable concrete production. However, the findings are limited to the defined design space, and further studies are required to confirm microstructural mechanisms and long-term durability. This study provides a replicable framework for the design and optimization of sustainable multi-component binder systems.

References

Althoey, F. (2023). Impact of nano-silica on the hydration, strength, and durability of concrete. *Construction and Building Materials, 367*, 130321. https://doi.org/10.1016/j.conbuildmat.2023.130321

Bheel, N., Ali, M. O. A., Shafiq, N., Almujibah, H. R., Awoyera, P. O., & Kirgiz, M. S. (2023). Utilization of millet husk ash as a supplementary cementitious material in eco-friendly concrete: RSM modelling and

optimization. *Structures, 54*, 100–112. https://doi.org/10.1016/j.istruc.2023.05.012

British Standards Institution. (2019). *BS EN 12390-3: Testing hardened concrete—Part 3: Compressive strength of test specimens*. BSI.

Cornell, J. A., & Piepel, G. F. (2022). *Mixture experiments: Design and analysis* (4th ed.). Wiley.

Du, H., & Pang, S. D. (2018). Properties of cement mortar containing high volume of calcium carbide residue. *Construction and Building Materials, 163*, 719–728. https://doi.org/10.1016/j.conbuildmat.2017.12.156

Juenger, M. C. G., Winnefeld, F., Provis, J. L., & Ideker, J. H. (2011). Advances in alternative cementitious binders. *Cement and Concrete Research, 41*(12), 1232–1243. https://doi.org/10.1016/j.cemconres.2010.11.012

Le, V. H., Thuc, C. N. H., & Thuc, H. H. (2013). Synthesis of silica nanoparticles from rice husk by sol–gel method. *Nanoscale Research Letters, 8*, 58. https://doi.org/10.1186/1556-276X-8-58

Myers, R. H., Montgomery, D. C., & Anderson-Cook, C. M. (2022). *Response surface methodology: Process and product optimization using designed experiments* (5th ed.). Wiley.

Ogunbode, E. B., Gajere, D., Hassan, I. O., John, A., Musa, S., & Nimlyat, P. S. (2021). Impact resistance properties of rice husk ash-based kenaf fibrous concrete. *Architecture Journal, 4*(2), 56–65.

Oritola, S. F. (2024). Production and characterization of pearl millet husk ash as a pozzolan. *Nile Journal of Engineering and Applied Sciences, 1*(1), 1–7.

Rong, Z., Sun, W., Xiao, H., & Jiang, G. (2020). Effects of nano-SiO_2 on the properties of high-performance concrete. *Materials, 13*(5), 1105. https://doi.org/10.3390/ma13051105

Said, A. M., Zeidan, M. S., Bassuoni, M. T., & Tian, Y. (2012). Properties of concrete incorporating nano-silica. *Construction and Building Materials, 36*, 838–844. https://doi.org/10.1016/j.conbuildmat.2012.06.044

Scrivener, K. L., John, V. M., & Gartner, E. M. (2018). Eco-efficient cements: Potential economically viable solutions for a low-CO_2 cement-based materials industry. *Cement and Concrete Research, 114*, 2–26. https://doi.org/10.1016/j.cemconres.2018.03.015

Shaikh, F. U. A., & Hosan, A. (2019). Effect of nano silica on compressive strength and microstructure of blended pastes. *Sustainable Materials and Technologies, 19*, e00111. https://doi.org/10.1016/j.susmat.2019.e00111

Stat-Ease, Inc. (2021). *Design-Expert® software (Version 13)* [Computer software]. https://www.statease.com

Yang, L., Jia, Z., Zhang, Y., & Dai, J. (2021). Effects of calcium carbide residue on cement-based materials. *Construction and Building Materials, 271*, 121878. https://doi.org/10.1016/j.conbuildmat.2020.121878

Zhang, P. (2022). Review of the role of nano-silica in cement-based materials. *Nanomaterials, 12*(5), 857. https://doi.org/10.3390/nano12050857